VOLUME 69, NUMBER 19 PHYSICAL REVIEW LETTERS 9 NOVEMBER 1992

Structure of High-T_c Superlattices

Eric E. Fullerton,[a] J. Guimpel,[b] O. Nakamura,[c] and Ivan K. Schuller
Physics Department, 0319, University of California, San Diego, La Jolla, California 92093-0319
(Received 24 April 1992)

We have determined the structure of $YBa_2Cu_3O_x/PrBa_2Cu_3O_x$ and $YBa_2Cu_3O_x/GdBa_2Cu_3O_x$ high-T_c superlattices using a novel method to refine the structure from x-ray diffraction spectra. This technique allows quantitative determination of disorder in superlattices in good agreement with independent measurements where available. The results show that layer thickness fluctuations, interdiffusion, and strains are present in the high-T_c superlattices and cannot be neglected when studying the physical properties.

PACS numbers: 74.75.+t, 61.10.My, 68.65.+g

Artificially layered systems have been extensively used for the study of dimensionality and proximity effect in conventional superconductors [1]. Recently, superlattices of high-T_c oxides, especially $YBa_2Cu_3O_x/PrBa_2Cu_3O_x$ (YBCO/PrBCO) [2–4], attracted much attention due to the possibility of studying a variety of phenomena otherwise inaccessible. One of the many interesting characteristics of this system is the reduction of T_c observed for thin YBCO layers separated by PrBCO layers. Several theoretical models have been proposed to account for this T_c suppression, including a spin polaron model [5], Kosterlitz-Thouless transition [6], and proximity effect [7]. These theories do not take into account possible disorder at the interfaces (interdiffusion, steps, strain, etc.), and assume perfect layering. On the other hand, superlattices of bismuth-based compounds show opposite results; superconductor/semiconductor superlattices of $Bi_2Sr_2CaCu_2O_8/Bi_2Sr_2CuO_6$ [8] and the $Bi_2Sr_2(Ca_{1-x}Y_x)Cu_2O_8$ system [9] show no observable suppression of T_c by the artificial layering. Recently, it was pointed out [10] that the suppression of T_c found in YBCO/PrBCO superlattices may be extrinsic, due to the interdiffusion between Y and Pr sites and interfacial strain. It is clear that the structural and chemical properties of these artificial structures are of extreme importance for the interpretation of the results. Layer thickness fluctuations may affect the superconducting properties [11]; in the case of YBCO/PrBCO superlattices interdiffusion will affect the T_c of the system given that; alloying with Pr is known to affect T_c in bulk $RBa_2Cu_3O_x$ (RBCO) oxides [12] and strains affect the properties by modifying the interatomic distances within the unit cell [13].

To date the structural analysis of high-T_c superlattices has been carried out mainly using *qualitative* interpretation of high-resolution transmission electron microscopy (HRTEM) [14,15] or x-ray diffraction (XRD). HRTEM has successfully identified steps of one unit cell in the layer thickness and long-range undulations in the overall structure although its somewhat limited by the extensive sample preparation, studies a local sample area, cannot resolve small lattice strains, and does not give conclusive results regarding interdiffusion. XRD is a complementary technique, which is nondestructive, averages over the entire film, and gives structural information on the atomic scale.

In this Letter, we present a *quantitative* structural analysis of YBCO/PrBCO and YBCO/GdBCO superlattices by XRD. This analysis, based on the refinement of the structure from XRD spectra, allows the introduction of disorder and gives quantitative information on the interfacial structure. The results show that layer thickness fluctuations, interdiffusion between the trivalent ions, and strains play an important role in the superlattice structure.

The samples were grown by dc magnetron sputtering using a technique described previously [16]. To the best of our knowledge this is the first preparation technique which produced samples that exhibit a large number of clear finite-size peaks for thin high-T_c films showing one unit cell uniformity in thickness. The samples were deposited from stoichiometric oxide targets on polished (100) $SrTiO_3$ (STO) and thermally annealed (100) MgO substrates at $\approx 700\,^{\circ}C$ for YBCO/GdBCO and $\approx 750\,^{\circ}C$ for YBCO/PrBCO, respectively. All films show nearly perfect c-texture growth in standard θ-2θ XRD spectra using Cu $K\alpha$ radiation. Typical FWHM of rocking curve scans about (00l) Bragg peaks are 0.3°–0.7° for YBCO/GdBCO on MgO, 0.1°–0.2° for YBCO/PrBCO on STO, and 0.4°–1.0° for YBCO/PrBCO on MgO. The structural data are comparable to others published in the literature, indicating that the quality of the superlattices is as high as any shown in the published literature. The YBCO/GdBCO superlattices show sharp resistive transitions (~1–3 K) with high onset temperature (~85–90 K) and basically no dependence on the layer thickness, as expected [11]. The transitions of YBCO/PrBCO superlattices show similar trends and values as those observed previously by other groups [2,3]. The results presented here are based on detailed structural analysis of about fifteen superlattices.

Figure 1(b) shows the measured x-ray diffraction spectrum of a representative YBCO(1 uc)/PrBCO(8 uc) superlattice grown on MgO. The spectrum consists of the (00l) peaks resulting from the periodicity of the high-T_c

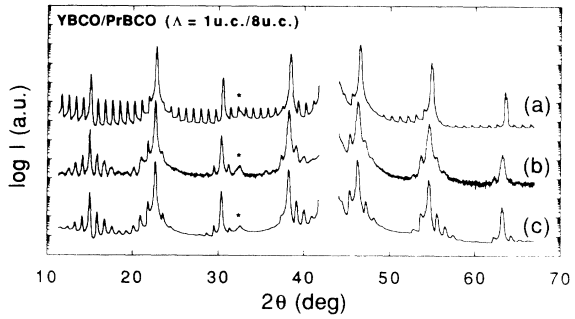

FIG. 1. θ-2θ x-ray spectra for a 2000-Å-thick YBCO (1 unit cell)/PrBCO (8 unit cells) superlattice. (a) Perfect superlattice simulation, (b) experimental data, and (c) refined spectrum. The spectra were offset by three decades and the MgO substrate peak was deleted for clarity. The asterisk indicates a small peak corresponding to the (110) diffraction.

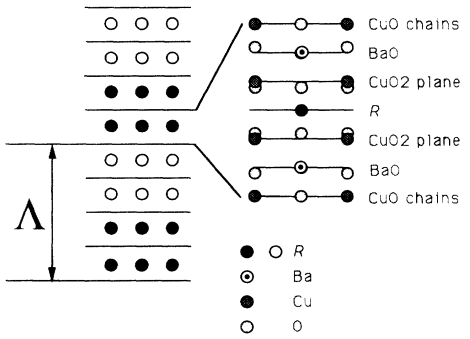

FIG. 2. Model for the perfect superlattice. White and black dots indicate the position of the two alternating trivalent ions. Lines indicate the limits of the unit cells, whose structure is described as layers of CuO, BaO, CuO_2, and R with the proper interatomic spacing and oxygen positions. For the unit cell schematic drawing the lines indicate the atomic plane position.

unit cell (uc), and satellite peaks about each (00l) peak from the modulation on the rare-earth site out to the (008) reflections. The only quantities which can be directly determined from the peak positions are the average c-axis length from the (00l) positions and the modulation wavelength (Λ) from the separation of the satellite peaks. The width of the (00l) diffraction peaks gives an estimate of the crystalline coherence length which is greater than 1000 Å for all of our superlattices.

To obtain additional information about the structure of the constituent layers requires a detailed quantitative comparison of calculated and measured intensities as previously described and thoroughly tested [17]. The method is similar to standard structural refinement techniques used for many years for complex oxides [18,19], where different disorder mechanisms are also included in the structural model. Figure 2 shows schematically the model used to describe a perfect c-oriented RBCO-based superlattice. The interplanar distances between metal ions are used as refinable parameters to account for possible strains. The calculated spectra include $K\alpha_1$-$K\alpha_2$ splitting and are convoluted with a Gaussian of width 0.05° to correct for the instrumental resolution. Line shapes are determined by the structural model which allows for refinement of the entire diffraction spectra. The sample-independent parameters included in the refinement are a scaling factor, a constant background, and a general line profile for the substrate peak.

In order to check that the model is describing properly the structure, we have refined the spectra of single RBCO (R=Y,Pr,Dy,Gd,Yb) films. In all cases, the model described quantitatively *both* the relative peak intensity and peak shape, typically over more than 4 orders of magnitude. The interplanar distances are within 0.02 Å of the bulk value (see Table I).

Figure 1(a) shows the result of a calculation assuming a perfect superlattice. Although the calculated spectra have the same qualitative features as the measured ones, it is clear there are a number of discrepancies in both the linewidths and relative intensities of the satellite peaks. In general, the measured satellite peaks are much broader and have lower intensities than the simulated spectra. Clearly disorder is present in these superlattices.

A quantitative comparison of measured intensities with model calculations requires including disorder into the structural model and deviation of the unit cell lattice spacing from bulk values. Defects in the crystal structures such as stacking faults limit crystal coherence and broaden all diffraction peaks. Given the long-range crystalline coherence, this type of disorder appears to be limited. To account for any loss of crystalline order, the model includes small continuous Gaussian fluctuations of layer thicknesses which limit long-range crystalline coherence [17].

Other parameters which may affect the satellite peaks relate to the ordering of the rare-earth sites. Interdiffusion of the rare-earth sites results from the random mixing of the rare-earth atoms across the interface or short-range random lateral steps in the interface. Steps in the layers which occur over long-range lateral distances result in discrete fluctuations in layer thickness in the growth direction. These two types of disorder produce different effects over the x-ray spectra. Interdiffusion modifies the interface profile but not its position and affects the superlattice peak intensities but not their width. Layer thickness fluctuations modify the local periodicity of the superlattice and therefore affect both the superlattice peak intensity and width. Broadening of the satellite peaks increases with increased order from the (00l) peak. Since interdiffusion and discrete disorder do not affect the crystalline order of the superlattice they have limited effect on the linewidth of the (00l) diffraction peaks.

The results of the refinement procedure in Fig. 1(c) shows that both the relative intensities and linewidths of

TABLE I. Refinement parameters for selected high-T_c films and superlattices. $\bar{N}$ is the average number of unit cells (uc) for a constituent layer. Cu(1)-Ba, Ba-Cu(2), and Cu(2)-R are the interplanar spacings separating the metal ions above the c axis as shown in Fig. 2. For the superlattices, the top number is for the YBCO layer and the bottom number is the GdBCO or PrBCO layer. Numbers in the parentheses indicate uncertainties in the last digit estimated from the fluctuation in refinement results on different initial parameters and details of the refinement model. Discrete disorder and interdiffusion parameters are discussed in the text. Bulk values for YBCO and GdBCO are from Ref. [13] and for PrBCO, from Ref. [21]. R_{wp} and R_e are defined as $\{\sum_i w_i[I_{m,i}-I_{c,i}]^2/\sum_i w_i[I_{m,i}]^2\}^{1/2}$ and $\{(N_p-N_f)/\sum_i w_i[I_{m,i}]^2\}^{1/2}$, respectively, where the sum runs over all (N_p) the data points, I_m and I_c are the measured and calculated intensities, respectively, w_i is a weighting factor that equals $1/I_{m,i}$ for Poisson statistics, and N_f is the number of free variables in the fit.

Sample	$\bar{N}$(uc)	Cu1-Ba (Å)	Ba-Cu2 (Å)	Cu2-R (Å)	c-axis (Å)	R_{wp}	R_e
YBCO Bulk	-	2.147	1.994	1.697	11.676	-	-
GdBCO Bulk	-	2.143	1.987	1.717	11.694	-	-
PrBCO Bulk	-	2.133	1.965	1.761	11.718	-	-
YBCO Film	-	2.15 (1)	2.01 (1)	1.70 (1)	11.722 (3)	0.29	0.08
GdBCO Film	-	2.14 (1)	2.01 (1)	1.72 (1)	11.746 (3)	0.26	0.08
PrBCO Film	-	2.13 (1)	1.99 (1)	1.78 (1)	11.800 (3)	0.32	0.03
Y(4uc)/Gd(4uc)	4.4	2.15 (1)	2.03 (2)	1.67 (2)	11.70 (1)	0.26	0.01
	3.7	2.15 (1)	2.00 (2)	1.73 (2)	11.76 (1)		
Y(1uc)/Gd(1uc)	1.1	2.16 (1)	2.04 (2)	1.64 (2)	11.68 (1)	0.37	0.01
	0.9	2.15 (1)	1.99 (2)	1.75 (2)	11.78 (1)		
Y(1uc)/Pr(8uc)	1.0	2.17 (1)	1.99 (3)	1.65 (2)	11.63 (1)	0.33	0.03
	7.8	2.13 (1)	1.99 (1)	1.78 (1)	11.80 (1)		
Y(1uc)/Pr(2uc)	1.0	2.16 (1)	2.03 (1)	1.65 (1)	11.69 (2)	0.38	0.03
	2.0	2.14 (1)	1.98 (1)	1.78 (1)	11.80 (1)		

all peaks are quantitatively reproduced [20]. Table I gives the refined values for interplanar distances and average layer thicknesses for several superlattices. The continuous roughness parameters for the superlattices and thin films were equivalent, indicating that there was no increase in defects in the crystalline structure in going from a single film to a superlattice. For both the YBCO/PrBCO and YBCO/GdBCO superlattices, the discrete disorder was 1 unit cell. That is, for a 1 unit cell layer, there is a finite probability of having 0 or 2 unit cells. In all cases, more than 90% of the layer thickness distributions were confined with 1 unit cell of the average. The interdiffusion in the first interfacial unit cell is approximately 15% Pr or Gd in the Y sites for YBCO layer thicknesses greater than 1 unit cell which is close to the limits of resolution of 10% obtained in z-contrast HRTEM [15]. This increases to approximately (25–30)% $\pm$ 5% for a single unit cell layer which is consistent with interdiffusion occurring across both interfaces for a single YBCO unit cell superlattice.

The a and b lattice parameters which depend on the rare earth result in interfacial epitaxial strains modifying both the in- and out-of-plane lattice parameters. As a result of interdiffusion and strains at the interface, the interplanar spacings change with decreasing layer thickness. Since the in-plane lattice areas for GdBCO and PrBCO are (1–2)% larger than YBCO, the *in-plane* strains on the YBCO layers should be expansive giving rise to an *out-of-plane* compression as observed in the refinement results. In all cases, the YBCO c-axis length is contracted with respect to the thin film value. With increasing PrBCO layer thickness a constant YBCO layer will accommodate more of the in-plane epitaxial strains which results in a contraction of the YBCO c-axis lattice parameter. This effect is clearly observed in Fig. 3 as the YBCO contracts for increased PrBCO layer thickness. It should be realized that changes in the structure of superlattices may occur either by surface or bulk diffusion during growth. This is especially true for the short length scales considered here. The only other technique capable

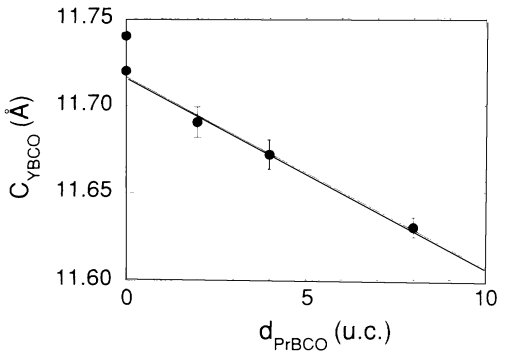

FIG. 3. c-axis lattice parameter for YBCO in a YBCO(1 unit cell)/PrBCO(d_{PrBCO}) superlattice 2000 Å thick as a function of d_{PrBCO}.

of determining the structure at these length scales, after the growth, is HRTEM. To the best of our knowledge a detailed, quantitative comparison of experimental images and model calculations has not been carried out for this technique. However, as stated above, our results on interdiffusion are compatible with the published literature [15] within the experimental resolution.

In conclusion, we have refined the structure of RBCO-based high-T_c thin films and superlattices. We have found that there are clear effects of layer thickness fluctuations, interdiffusion, and strains in the x-ray spectra which cannot be neglected. These effects must be taken into account in any model that interprets the physical properties of these materials.

This work was supported by the Office of Naval Research Grant No. N00014-91J-1438. Some international travel for J.G. was provided through a fellowship from CONICET, Argentina. We thank Professor K. Kitazawa and Dr. T. Izumi for arranging the Tonen-UCSD collaboration.

[a]Present address: Materials Science Division, Argonne National Laboratory, Argonne, IL 60439.

[b]On leave from Centro Atómico Bariloche, 8400 Bariloche, Argentina.

[c]Permanent address: Tonen Corporation, 1-3-1 Nishi-Tsurugaoka, Ohi-Machi, Iruma-Gun, Saitama 354, Japan.

[1] See, for instance, I. K. Schuller, in *Physics, Fabrication and Applications of Multilayered Structures*, edited by P. Dhez and C. Weisbuch (Plenum, New York, 1988).

[2] J.-M. Triscone, Ø. Fischer, O. Brunner, L. Antognazza, A. D. Kent, and M. G. Karkut, Phys. Rev. Lett. **64**, 804 (1990).

[3] Q. Li, X. X. Xi, X. D. Wu, A. Inam, S. Valdlamannati, W. L. McLean, T. Venkatesan, R. Ramesh, D. M. Hwang, J. A. Martinez, and L. Nazar, Phys. Rev. Lett. **64**, 3086 (1990).

[4] D. H. Lowndes, D. P. Norton, and J. D. Budai, Phys. Rev. Lett. **65**, 1160 (1990).

[5] R. F. Wood, Phys. Rev. Lett. **66**, 829 (1991).

[6] M. Rasolt, T. Edis, and Z. Tesanovic, Phys. Rev. Lett. **66**, 2927 (1991).

[7] J. Z. Wu, C. S. Ting, W. K.Chu, and X. X. Yao, Phys. Rev. B **44**, 411 (1991).

[8] K. Horiuchi, T. Kawai, M. Kanai, and S. Kawai, Jpn. J. Appl. Phys. **30**, L1381 (1991).

[9] M. Kanai, T. Kawai, and S. Kawai, Appl. Phys. Lett. **57**, 198 (1990).

[10] T. H. Geballe, in Proceedings of the Toshiba International School of Superconductivity (unpublished).

[11] I. N. Chan, D. C. Vier, O. Nakamura, J. Hasen, J. Guimpel, S. Schultz, and Ivan K. Schuller (unpublished).

[12] For an early report see, for instance, L. Soderholm, K. Zhang, D. G. Hinks, M. A. Beno, J. D. Jorgensen, C. U. Segre, and I. K. Schuller, Nature (London) **328**, 604 (1987).

[13] A. A. R. Fernandes, J. Santamaria, S. Bud'ko, O. Nakamura, J. Guimpel, and Ivan K. Schuller, Phys. Rev. B **44**, 7601 (1991).

[14] O. Eibl, H. E. Hoenig, J.-M. Triscone, Ø. Fischer, L. Antognazza, and O. Brunner, Physica (Amsterdam) **172C**, 365 (1990).

[15] S. J. Pennycook, M. F. Chisholm, D. E. Jesson, D. P. Norton, D. H. Lowndes, R. Feenstra, H. R. Kerchner, and J. O. Thomson, Phys. Rev. Lett. **67**, 765 (1991).

[16] O. Nakamura, Eric E. Fullerton, J. Guimpel, and Ivan K. Schuller, Appl. Phys. Lett. **60**, 120 (1992).

[17] Eric E. Fullerton, Ivan K. Schuller, H. Vanderstraeten, and Y. Bruynseraede, Phys. Rev. B **45**, 9292 (1992).

[18] H. M. Rietveld, J. Appl. Cryst. **2**, 65 (1969).

[19] For a review of structural refinement, see J. D. Jorgensen and J. Newsan, MRS Bull. **15**, 49 (1990).

[20] The superlattice spectra are usually fitted with fourteen adjustable parameters which include: three interatomic spacings, an average thickness, and a discrete layer thickness fluctuation for each material; interdiffusion, continuous fluctuation, constant baseline, and scaling factor. An additional four parameters describe the MgO substrate peak using $y=H\{1+[(x-x_0)/\Gamma]^{\tau}\}^{-1}$ where H, x_0, Γ, and τ are the height, center, width, and exponent, respectively, that define the line shape. $\tau=2$ corresponds to a Lorenztian line shape.

[21] *Physical Properties of High Temperature Superconductors II*, edited by D. M. Ginsberg (World Scientific, Singapore, 1990).

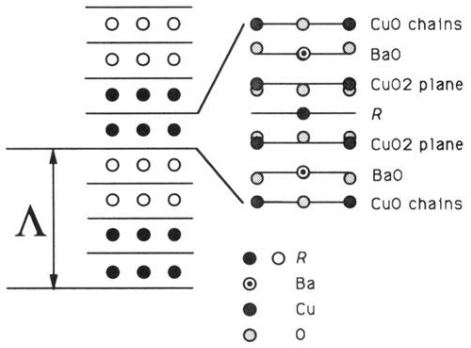

FIG. 2. Model for the perfect superlattice. White and black dots indicate the position of the two alternating trivalent ions. Lines indicate the limits of the unit cells, whose structure is described as layers of CuO, BaO, CuO_2, and R with the proper interatomic spacing and oxygen positions. For the unit cell schematic drawing the lines indicate the atomic plane position.